Comparative transcriptomics of extreme phenotypes of human HIV-1 infection and SIV infection in sooty mangabey and rhesus macaque

Rotger, M ; Dalmau, J ; Rauch, A ; McLaren, P ; Bosinger, S E ; Martinez, R ; Sandler, N G ; Roque, A ; Liebner, J ; Battegay, M ; Bernasconi, E ; Descombes, P ; Erkizia, I ; Fellay, J ; Hirschel, B ; Miró, J M ; Palou, E ; Hoffmann, M ; Massanella, M ; Blanco, J ; Woods, M ; Günthard, H F ; de Bakker, P ; Douek, D C ; Silvestri, G ; Martinez-Picado, J ; Telenti, A

Abstract: High levels of HIV-1 replication during the chronic phase of infection usually correlate with rapid progression to severe immunodeficiency. However, a minority of highly viremic individuals remains asymptomatic and maintains high CD4 T cell counts. This tolerant profile is poorly understood and reminiscent of the widely studied nonprogressive disease model of SIV infection in natural hosts. Here, we identify transcriptome differences between rapid progressors (RPs) and viremic nonprogressors (VNPs) and highlight several genes relevant for the understanding of HIV-1-induced immunosuppression. RPs were characterized by a specific transcriptome profile of CD4 and CD8 T cells similar to that observed in pathogenic SIV-infected rhesus macaques. In contrast, VNPs exhibited lower expression of interferon-stimulated genes and shared a common gene regulation profile with nonpathogenic SIV-infected sooty mangabeys. A short list of genes associated with VNP, including CASP1, CD38, LAG3, TNFSF13B, SOCS1, and EEF1D, showed significant correlation with time to disease progression when evaluated in an independent set of CD4 T cell expression data. This work characterizes 2 minimally studied clinical patterns of progression to AIDS, whose analysis may inform our understanding of HIV pathogenesis.

DOI: https://doi.org/10.1172/JCI45235

Comparative transcriptomics of extreme phenotypes of human HIV-1 infection and SIV infection in sooty mangabey and rhesus macaque

Margalida Rotger,[1] Judith Dalmau,[2] Andri Rauch,[3] Paul McLaren,[4] Steven E. Bosinger,[5] Raquel Martinez,[1] Netanya G. Sandler,[6] Annelys Roque,[6] Julia Liebner,[6] Manuel Battegay,[7] Enos Bernasconi,[8] Patrick Descombes,[9] Itziar Erkizia,[2] Jacques Fellay,[1] Bernard Hirschel,[10] Jose M. Miró,[11] Eduard Palou,[12] Matthias Hoffmann,[13] Marta Massanella,[2] Julià Blanco,[2] Matthew Woods,[14] Huldrych F. Günthard,[15] Paul de Bakker,[4] Daniel C. Douek,[6] Guido Silvestri,[5] Javier Martinez-Picado,[2,16] and Amalio Telenti[1,17]

[1]Institute of Microbiology, University Hospital and University of Lausanne, Lausanne, Switzerland. [2]AIDS Research Institute (IrsiCaixa), Hospital Universitari Germans Trias i Pujol, Badalona, Barcelona, Spain. [3]Division of Infectious Diseases, University Hospital Bern, Bern, Switzerland. [4]Division of Genetics, Brigham and Women's Hospital, Harvard Medical School, Boston, Massachusetts, USA. [5]Yerkes National Primate Research Center and Emory Vaccine Center, Emory University, Atlanta, Georgia, USA. [6]Human Immunology Section, Vaccine Research Center, National Institute of Allergy and Infectious Diseases, NIH, Bethesda, Maryland, USA. [7]Division of Infectious Diseases and Hospital Epidemiology, University Hospital Basel, Basel, Switzerland. [8]Ospedale Regionale, Lugano, Switzerland. [9]Genomics Platform, University of Geneva, Geneva, Switzerland. [10]Division of Infectious Diseases, University Hospital Geneva, Geneva, Switzerland. [11]Hospital Clinic — Institut d'Investigacions Biomèdiques August Pi i Sunyer, University of Barcelona, Barcelona, Spain. [12]Banc de Sang i Teixits, Barcelona, Spain. [13]Kantonsspital St. Gall, Saint Gallen, Switzerland. [14]Ragon Institute of MGH, MIT and Harvard, Boston, Massachusetts, USA. [15]Division of Infectious Diseases and Hospital Epidemiology, University Hospital Zurich, University of Zurich, Zurich, Switzerland. [16]Institució Catalana de Recerca i Estudis Avançats, Barcelona, Spain. [17]Swiss HIV Cohort Study (SHCS), Lausanne, Switzerland.

High levels of HIV-1 replication during the chronic phase of infection usually correlate with rapid progression to severe immunodeficiency. However, a minority of highly viremic individuals remains asymptomatic and maintains high CD4$^+$ T cell counts. This tolerant profile is poorly understood and reminiscent of the widely studied nonprogressive disease model of SIV infection in natural hosts. Here, we identify transcriptome differences between rapid progressors (RPs) and viremic nonprogressors (VNPs) and highlight several genes relevant for the understanding of HIV-1–induced immunosuppression. RPs were characterized by a specific transcriptome profile of CD4$^+$ and CD8$^+$ T cells similar to that observed in pathogenic SIV-infected rhesus macaques. In contrast, VNPs exhibited lower expression of interferon-stimulated genes and shared a common gene regulation profile with nonpathogenic SIV-infected sooty mangabeys. A short list of genes associated with VNP, including *CASP1*, *CD38*, *LAG3*, *TNFSF13B*, *SOCS1*, and *EEF1D*, showed significant correlation with time to disease progression when evaluated in an independent set of CD4$^+$ T cell expression data. This work characterizes 2 minimally studied clinical patterns of progression to AIDS, whose analysis may inform our understanding of HIV pathogenesis.

Introduction

HIV infection leads to severe immunodeficiency in most infected subjects, in an average of 10 years; however, there are marked departures from this estimate. Attention has been directed at understanding the determinants of nonprogressive disease, as exemplified by the clinical course of long-term nonprogressors and of elite controllers (1–3). The other extreme of the spectrum of disease — rapid progression — has been the subject of much less research. Rapid progressors (RPs) can be defined by a number of criteria — generally including progressive immunosuppression soon after seroconversion and, in many cases, high levels of viremia (4, 5). Limited data suggest that the concurrence of viral and host factors contributes to the severity of early disease (6). There are, however, few such individuals in clinical cohorts — the main limitations for prospective recruitment are the need to identify patients with a known date of infection (seroconverters), and the short window of clinical observation before antiretroviral treatment is initiated. These constrain the availability of relevant biological material for study.

There are also very rare individuals that can tolerate very high viral loads, comparable to those of RPs, while maintaining stable CD4$^+$ T cell counts for many years in the absence of treatment. Choudhary et al. (7) described 3 HIV-infected individuals with long-term asymptomatic disease who maintained stable CD4$^+$ T cell counts and low levels of immune activation, despite viral replication in the range of 10^4 to 10^5 HIV-1 RNA copies per ml of plasma. This profile of tolerance of viral replication is reminiscent of the pattern of SIV infection in the natural host. The importance of such model for the understanding of HIV/AIDS pathogenesis has been underscored by

Authorship note: Margalida Rotger, Judith Dalmau, Andri Rauch, Paul McLaren, and Steven E. Bosinger contributed equally to this work.

Conflict of interest: The authors have declared that no conflict of interest exists.

Citation for this article: *J Clin Invest.* 2011;121(6):2391–2400. doi:10.1172/JCI45235.

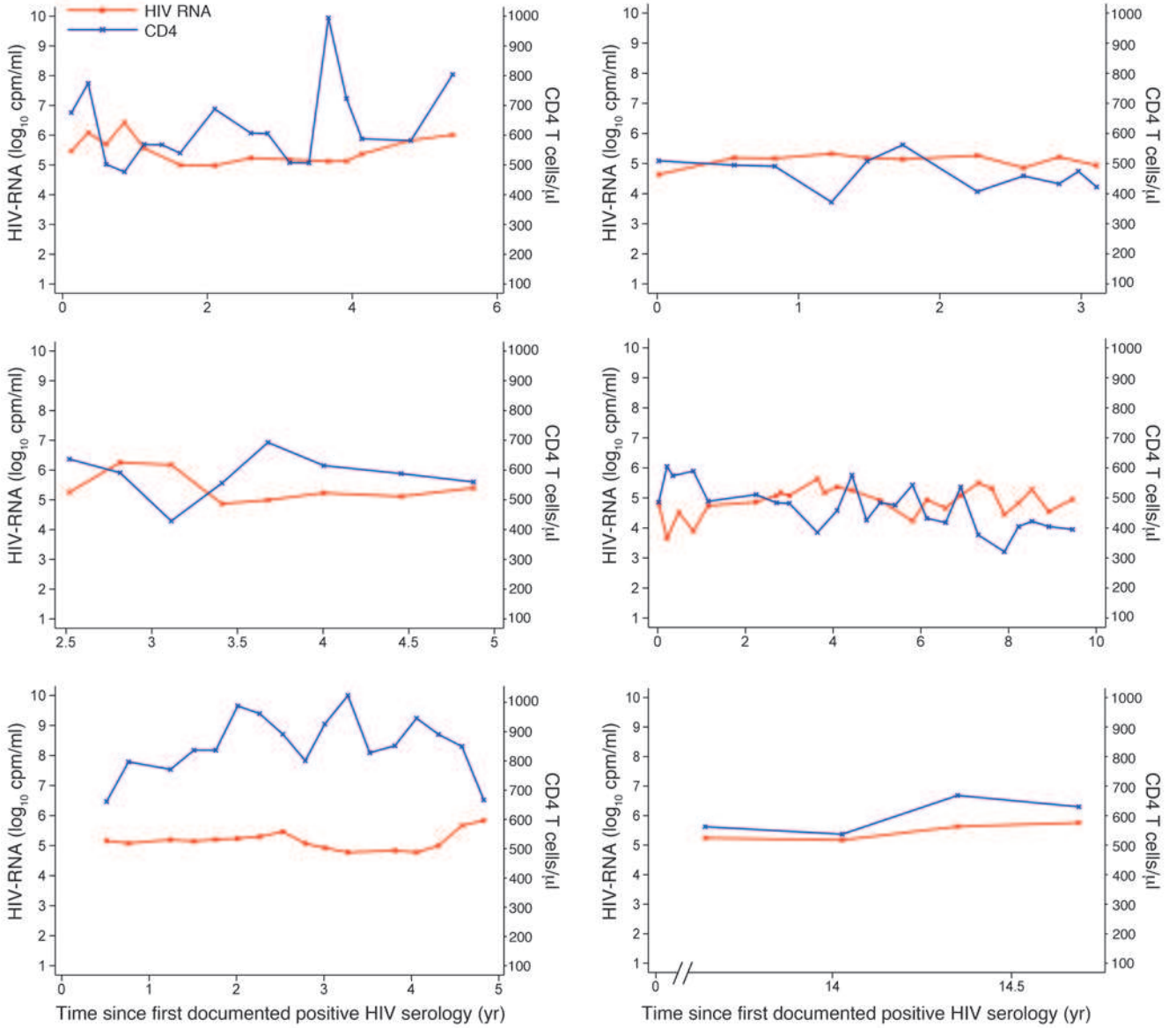

Figure 1
Individual viral loads and CD4+ T cell profiles of VNPs. Viremia is shown in red, and CD4+ T cell count is shown in blue.

studies in sooty mangabeys and in African green monkeys (8–12). Sooty mangabeys have nonprogressive disease despite chronic virus replication that is characterized by low levels of immune activation, while pathogenic SIV infection of rhesus macaques is associated with chronic immune activation. The consequences of immune activation include increased cell turnover, the skewing of lymphocytes toward more activated and differentiated subpopulations, and the induction of cellular exhaustion, senescence, and low renewal potential (reviewed in ref. 13).

The first goal of the present study was to explore a set of standard criteria to identify HIV-infected individuals presenting those 2 distinct clinical patterns: rapid progression and the contrasting setting of nonprogressive disease, despite prolonged and very high levels of viremia (extreme viremic nonprogressors [VNPs]). We then used immunogenetic, genomic, and transcriptomic tools and biomarkers to identify differences between those extreme groups as well as exploring genomic patterns previously defined in comparative studies of SIV infection in the pathogenic and the nonpathogenic models of rhesus macaques and sooty mangabeys, respectively (8–10). The study revealed characteristic biomarker and transcriptome patterns and highlighted several genes of relevance for the understanding of pathogenesis of HIV-1–induced immunosuppression.

Results

Clinical and immunogenetic profiles. We identified 6 individuals that fulfilled strict clinical criteria of VNPs and had material available for analysis; plots of the infection course for each VNP individual are shown in Figure 1. We further identified 66 individuals who fulfilled the criteria of rapid progression and had materials available for study; the collective plot is shown in Figure 2. Notably, at

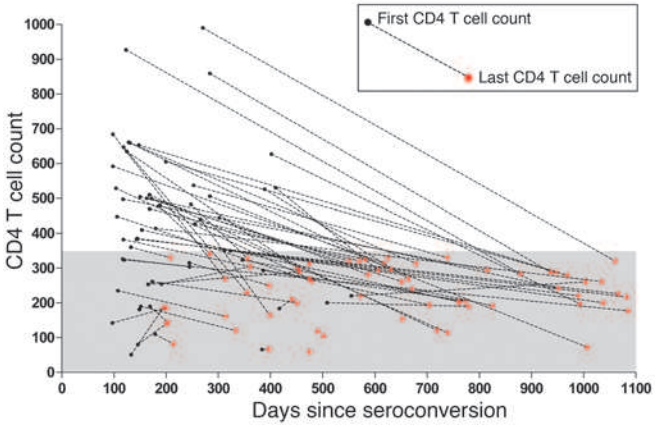

Figure 2
Evolution of T cell count in individuals with a profile of rapid progression. The first CD4+ T cell count determination (black symbols) and the last CD4+ T cell count determination (red symbols) (connected by dashed lines) in individuals, defined by the progression to fewer than 350 CD4+ T cells (denoted by the gray area) in fewer than 3 years after seroconversion. Only values beyond the 3-month window after seroconversion are considered.

the time of analysis, VNPs had higher levels of viral replication (set point HIV RNA, 5.4 $\log_{10}$ cp/ml; interquartile range [IQR], 5.1–5.5 $\log_{10}$ cp/ml]) compared with those of RPs (set point HIV RNA, 4.7 $\log_{10}$ cp/ml [IQR, 4.3–5.2 $\log_{10}$ cp/ml]). Transcriptome analysis also included 9 elite/viremic controllers (ECs) and 5 chronic progressors, as previously defined (5). Patient characteristics are detailed in Supplemental Table 1 (supplemental material available online with this article; doi:10.1172/JCI45235DS1).

The HLA and KIR alleles were determined in all individuals, compared across clinical groups and compared to the allele frequencies of 1,609 participants of the SHCS (Supplemental Figure 1). Protective alleles were underrepresented, and risk alleles were more common in RPs compared with the general population. In contrast to HLA alleles, there was no depletion of protective KIR alleles or KIR/HLA combinations in RPs (Supplemental Figure 2). HLA alleles of VNPs are shown in Supplemental Table 2. To determine whether any common variants of very large effect could be implicated in mediating rapid progression, the study was completed with a genome-wide association across an approximately 500,000-loci study that included 66 RPs and 757 participants of the SHCS. No SNPs reached genome-wide significance (Supplemental Figure 3 and Supplemental Table 3), likely due to the limited power to detect anything other than very large effect sizes. A previous genome-wide association study of rapid progression (4) identified 8 SNPs that passed the study-wide false discovery rate (FDR) cutoff of 25%. These failed confirmation in our study (Supplemental Table 4).

Transcriptome analysis in CD4+ T cells. To investigate differences at the transcriptome level between RPs and VNPs, we performed microarray analysis on purified CD4+ cells from 27 RPs, 5 VNPs, 5 chronic progressors, and 9 ECs (Supplemental Table 1B). RPs, with and without transcriptome analysis, were similar with regard to CD4+ T cell counts and HIV viral load. The median CD4+ T cell counts at baseline were 440 cells/μl (IQR, 350–506 cells/μl) and 382 cells/μl (IQR, 315–497 cells/μl) for those with and without transcriptome analysis, respectively; the median baseline HIV viral loads were 4.8 cp/ml (IQR, 4.1–5.5 cp/ml) and 4.9 cp/ml (IQR, 4.3–5.1 cp/ml). During follow-up, the median CD4+ T cell counts were 263 cells/μl (IQR, 197–313 cells/μl) and 223 cells/μl (IQR, 186–299 cells/μl), and median HIV viral loads were 4.8 cp/ml (IQR, 4.3–5.4 cp/ml) and 5.0 cp/ml (IQR, 4.4–5.2 cp/ml) ($P > 0.4$ for all comparisons). Thirteen (20%) individuals had an AIDS-defining event within 3 years of seroconversion.

Principal component analysis identified 4 outliers that were excluded from further analysis. Various parameters were assessed as covariates (clinical center, gender, age, CD4+ T cell viability and laboratory date, and microarray chip batch); we retained chip batch as a statistically significant covariate. To contrast specific patient profiles, we applied a Bayesian approach to the analysis of gene expression (14). Analysis of RPs versus ECs identified 14 differentially expressed genes at a FDR-adjusted *P* value of less than 0.05. Interferon-stimulated genes (ISGs) are well known to be upregulated in patients with progressive HIV disease. Consistent with this knowledge, 6 ISGs, *IFI44* (and its ligand *IFI44L*), *MX1*, *EIF2AK2*, *IFI6*, *LY6E*, *TRIM22*, were upregulated in RPs. Other upregulated genes included *SYNCRIP* that encodes a nuclear ribonucleoprotein (hnRNP-Q) associated with the *APOB* mRNA editosome complex that may modulate the posttranscriptional C to U RNA-editing *PRIC285* that encodes a helicase acting as a transcriptional coactivator for a number of nuclear receptors, *EPSTI1* and *MRPS18B*. Genes downregulated in RPs included *TRK1*, which encodes a kinase, and *FOXJ2*, a transcriptional activator. Next, we specifically searched genes uniquely associated with the VNP profile by contrasting this profile with that of RPs or chronic progressors. This analysis failed to identify FDR-adjusted differentially expressed genes.

Transcriptome analysis in CD8+ T cells. We also performed microarray analysis on purified CD8+ T cells derived from the same PBMC samples used for CD4+ T cell transcriptome analysis. Expression analysis was successfully completed for 25 RPs and 5 VNPs as well as 5 chronic progressors and 8 elite and viremic controllers (Supplemental Table 1B). No outliers were identified, and all samples progressed to further analysis. As above, we retained microarray chip batch as covariate in all definitive analyses. Using the same sensitive Bayesian approach as for the CD4+ T cell analysis (14), contrasting of RPs and ECs yielded 317 differentially expressed genes at a FDR-adjusted *P* value less than or equal to 0.05 (Supplemental Table 5). Among the 180 genes upregulated in RPs, prominent groups of genes included multiple members of the proteasome and interferon-induced immunoproteasome, ISGs, and cell cycle, cell division, and metabolic genes indicating cell proliferation (Supplemental Figure 4). No apparent mechanisms were deduced from the collective analysis of 137 genes downregulated in RPs by using EMBL Search Tool for the Retrieval of Interacting Genes/Proteins (STRING), Ingenuity Pathway Analysis 7.0 (IPA), and KEGG pathway analysis (see Methods). As for the CD4+ T cells, we specifically searched genes uniquely associated with the VNP profile by contrasting this profile with that of RPs or chronic progressors. Given power limitations, this analysis failed to identify FDR-adjusted differentially expressed genes. Thus, we proceeded to the analysis of specific pathways and of the genes identified in primate studies of nonpathogenic SIV infection (9, 10).

Analysis of genes of the interferon response. Recent publications (8–12) highlight a distinctive downregulation of the interferon response after SIV infection of natural host species, such as sooty mangabeys and African green monkeys. In contrast, SIV infection of the pathogenic models of rhesus or pig-tailed macaque is character-

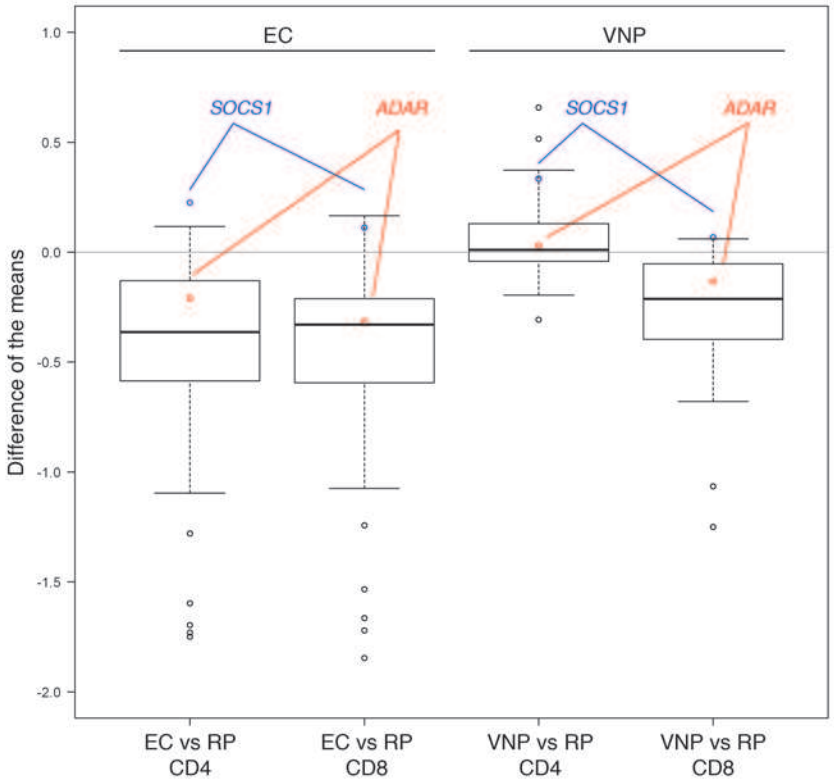

Figure 3
Analysis of differential expression of ISGs. Consistent with the primate natural infection model, a representative set of ISGs (n = 29) had lower expression levels in CD8+ T cells from VNPs than in those from RPs. The box-and-whisker plot indicates that the differences are more pronounced for the comparisons of ECs and RPs. The horizontal bars indicate the median values, the boxes indicate the 25th to 75th percentiles, and whiskers indicate extremes. Each dot represents the difference in expression value for a given gene across groups. The profiles of the inhibitor of interferon response, *SOCS1*, and of *ADAR* are highlighted (blue and red, respectively).

ized by persistence of deregulated interferon responses. Consistent with the primate model of natural infection, we observed a lower level of expression of ISGs (see Methods for the specific ISGs) in CD8+ T cells of individuals with a VNP profile in comparison with that of individuals with a RP profile (Figure 3) (difference of the means, median –0.21 [IQR, –0.05 to –0.40]; paired t test, $P = 0.014$). However, these differences were not observed in CD4+ T cells, (difference of the means, 0.01 [IQR, 0.13 to –0.04]; $P = 0.59$). As expected, more profound differences in expression of ISGs were found in the comparison between ECs and RPs (median –0.36 [IQR, –0.13 to –0.59], $P = 2.5 \times 10^{-5}$ in CD4+ T cells, and median –0.33 [IQR, –0.21 to –0.59], $P = 3.8 \times 10^{-6}$ in CD8+ T cells) (Figure 3). The expression of *SOCS1*, involved in a negative feedback loop in the regulation of signal transduction through the JAK/STAT5 pathway, was higher in CD4+ T and CD8+ T cells of VNPs and ECs compared with that of RPs; the differences were statistically significant for the comparison of ECs and RPs in CD4+ T cells ($P = 0.02$) (Figure 3). This trend was not observed for a second regulator, *ADAR*.

Gene set enrichment analysis of human VNPs and SIV-infected sooty mangabeys. To examine whether the phenotype maintained by VNPs and natural host species was due to a shared, underlying molecular mechanism, we used gene set enrichment analysis (GSEA) of the human transcriptome data sets with gene sets derived from the analysis of sooty mangabeys and rhesus macaques (9). GSEA tests the relative position of a collection of genes ("query gene set") within an independent, ranked data set ("reference gene set"). Because GSEA relies on an additive signal of multiple genes within a data set, it is less dependent on arbitrary cutoffs, such as fold change of specific P values, making its ability to detect an underlying process within transcriptome data potentially more sensitive than a "single-gene" approach using traditional statistics. The use of rank data rather than absolute intensity measurements in GSEA also affords greater flexibility to make comparisons between diverse gene-expression data (i.e., between tissues, species, or array platforms) (15).

As presented in Table 1 and in Supplemental Figure 5, the query set of ISGs identified as differentially expressed in the rhesus macaque was associated with enrichment in human RPs, although the P values were only consistent with a statistical trend. The CD8+ T cell expression data was particularly enriched for the ISGs; the data set comprised 15,879 nonredundant genes, and the lowest-ranked

Table 1
Analysis of gene sets of the primate model

	VNP vs. RP CD4 pre-ranked data set		VNP vs. RP CD8 pre-ranked data set	
Gene set	**ES**	***P* value**	**ES**	***P* value**
ISGs (RM)	–0.70	0.156	–0.85	0.089
IA (RM)	–0.69	0.141	–0.83	0.075
SM > RM chronic phase	0.98	0.010	–0.30	0.786
Random	0.28	0.910	–0.44	0.667

Enrichment of genes upregulated in sooty mangabeys (SMs) or rhesus macaques (RMs) after SIV infection was analyzed by GSEA in expression data sets derived from contrasting human HIV-infected RPs with VNPs. Positive enrichment scores (ES) indicate enrichment in the VNP phenotype, and negative scores indicate enrichment in the RP phenotype. "SM > RM" denotes genes that were upregulated in sooty mangabeys to a higher degree than in rhesus macaques. IA, immune activation genes.

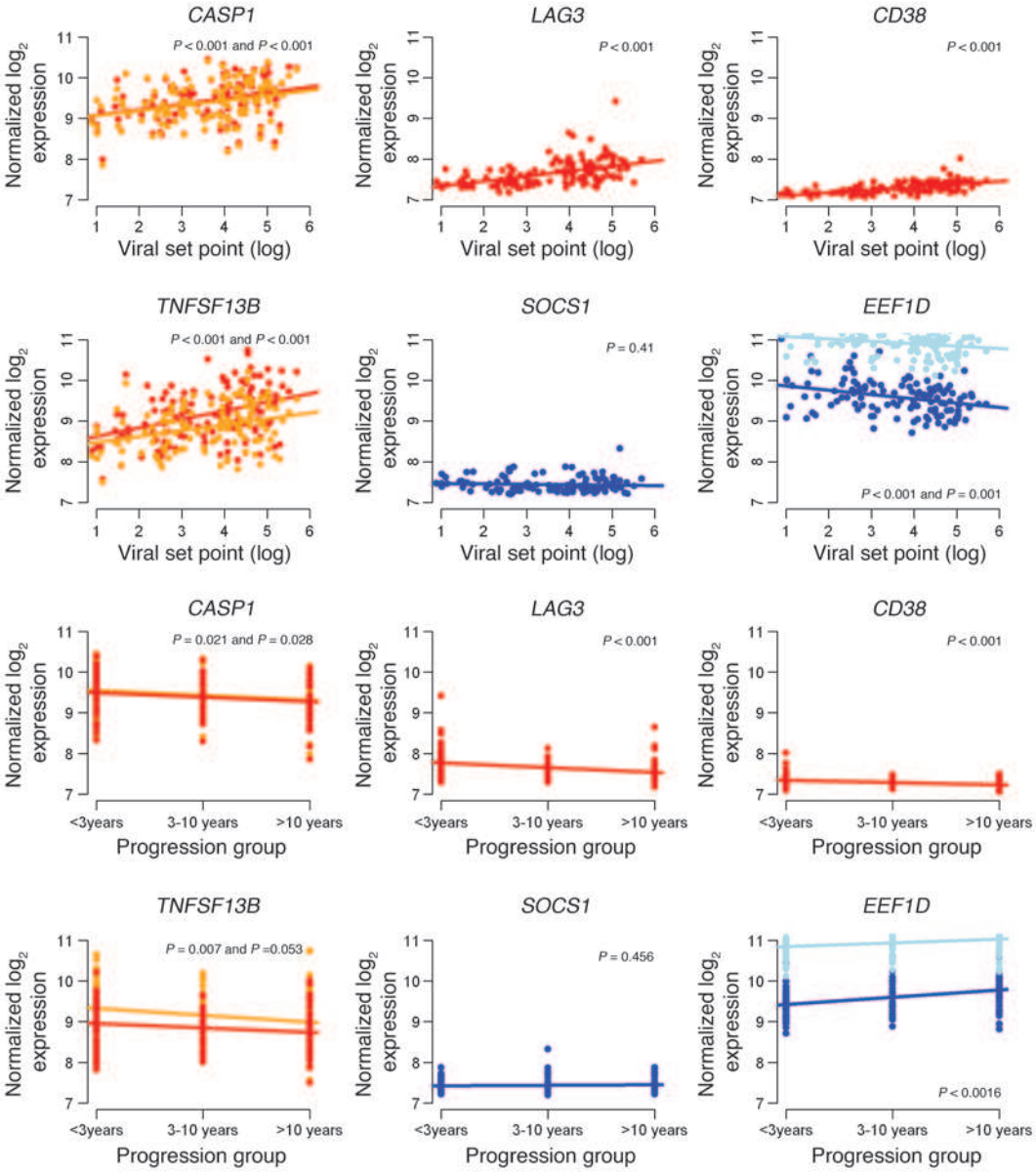

Figure 4

Analysis of the candidate VNP signature in an independent CD4+ T cell expression data set. The signature associated with the VNP profile upon transcriptome analysis in humans and nonhumans was tested in an independent validation set of 153 individuals, contributing CD4+ T cell expression data across all levels of viral set point after seroconversion. Correlations with individual gene expression levels and viral set point after seroconversion are shown in the 6 top panels. Correlations with disease progression, as indicated by time to CD4+ T cell count depletion to fewer than 350 cells/μl, are shown in the 6 bottom panels. Multiple probes for 1 gene are shown in different colors: orange/red is used for genes differentially upregulated in RPs, and blue/light blue is used for genes differentially upregulated in the VNPs. Where there are 2 *P* values, the first value represents the red/blue lines, and the second value represents the orange/light blue lines. Each dot represents an individual. The regression lines from the linear models are shown.

ISG was at position 10,562, well above the phenotype threshold at position 7,556, below which genes demonstrated higher expression in VNPs, and 12 out of 20 queried ISGs were higher than position 14,500 (Supplemental Figure 5). Genes found to be correlated with immune activation in rhesus macaques were also enriched in the RP phenotype in humans in both CD4 and CD8+ T cell data (Table 1 and Supplemental Figure 5). The enrichment of immune activation genes in RPs would indicate that VNPs have reduced cellular activation/proliferation relative to RPs. Taken together, these data suggest that VNPs, at least at the transcriptional level, are able to reduce the chronic immune activation seen in pathogenic HIV/SIV infection and that this attenuation largely overlaps with comparisons between sooty mangabeys and rhesus macaques. Because the human VNP and RP samples were obtained from the postacute phase of infection, we reasoned that genes found to be differentially expressed between sooty mangabeys and rhesus macaques during

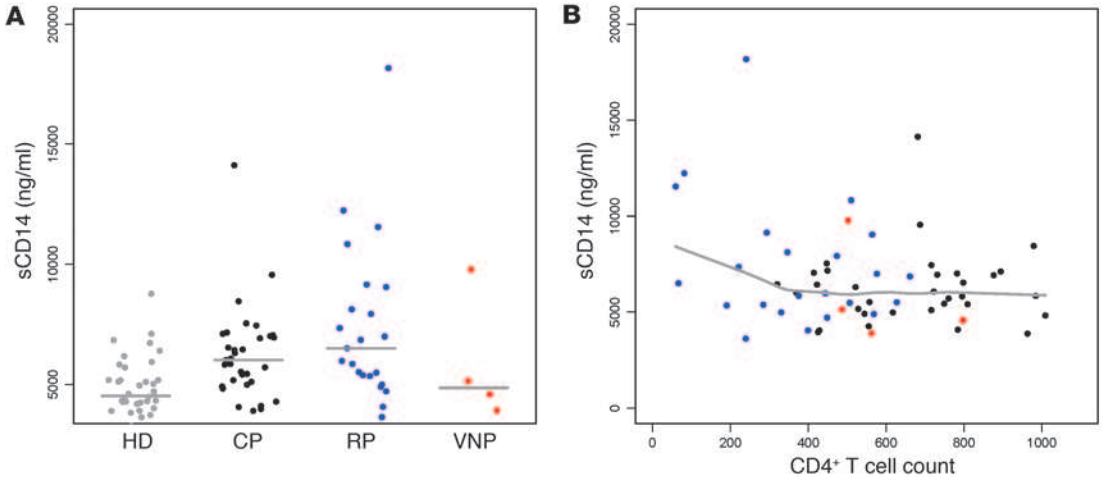

Figure 5
Analysis of sCD14 plasma levels. (**A**) sCD14 levels were measured during the 3-year period after seroconversion and/or transcriptome analysis in RPs (n = 24) and VNPs (n = 4). Chronic progressors (CP; n = 39) and healthy donors (HD; n = 38) contributed reference data. The gray line represents the median values. (**B**) RP sCD14 levels were higher at lower CD4+ T cell counts. The gray line represents the LOWESS curve fitted to the sample population. Each dot represents an individual

chronic infection may be enriched in the VNP phenotype. When we performed GSEA using genes found to be significantly higher in sooty mangabeys than rhesus macaques during chronic infection against the human data sets, we found that there was no significant enrichment in either phenotype in CD8+ T cells, but that there was significant enrichment in the VNP phenotype of CD4+ T cells (Table 1). The enrichment was largely driven by a single gene, *SV2A*, that ranked extremely high in the VNP phenotype. Taken together, these results suggest that sooty mangabeys and VNPs share some similarities in expression during chronic SIV/HIV infection; however, these similarities were not statistically significant.

Detailed analysis of genes identified in nonpathogenic primate models of natural infection. We extended the above analysis to examine in detail a list of genes reported by Bosinger et al. (9). We used a heuristic approach to inform this list (see Methods) by assessing (a) the consistency and direction of the association (downregulation or upregulation) between the primate model and the human expression profile, (b) the general correlation between CD4+ T cell and CD8+ T cell observations, and (c) the statistical support for the different associations in this subanalysis. Six genes fulfilled the criteria; genes *CASP1*, *CD38*, *LAG3*, and *TNFSF13B* presented lower expression levels in VNPs and in the nonpathogenic animal model, and *SOCS1* and *EEF1D* presented greater expression levels in VNPs and in the nonpathogenic animal model of infection. The short list of genes was constituted into a signature to be evaluated in an independent set of data. For this, we used the large data set of CD4+ T cell expression (16) to assess the association of the signature genes with viral load and with progression of immunosuppression (as defined by time to fewer than 350 CD4+ T cells/μl). In unadjusted regression, the following genes showed statistically significant association with time to progression to fewer than 350 CD4+ T cells/μl: *CASP1*, *LAG3*, *CD38*, *TNFSF13B*, and *EEF1D* (Figure 4). A multigene model explained 19.5% of the variance in disease progression (P = 0.0003). Inclusion of viral load in the model improved the proportion of variance explained to 26% ($P = 4.8 \times 10^{-7}$). However, there was significant colinearity with viral load and, after its inclusion in the model, only *EEF1D* remained as an independent variable (P = 0.013).

Association of soluble CD14 levels with clinical groups. To further assess whether the differences between RPs and VNPs reflected differences in mechanisms of pathogenesis, we assessed plasma levels of soluble CD14 (sCD14), which is produced by monocytes on becoming activated by LPS. Thus, plasma sCD14 levels reflect the host response to translocated bacterial products and are a significant independent predictor of mortality in HIV infection (17, 18). We analyzed samples from 24 RPs and 4 VNPs collected within 3 years after seroconversion. To contextualize these data, we measured plasma sCD14 levels in healthy volunteers and from chronic progressors. sCD14 levels were significantly higher in the plasma samples from RPs than in samples from chronic progressors, healthy donors, and for 3 out of 4 VNP samples analyzed (median 6,235 ng/ml [IQR, 5,069–8,808 ng/ml], median 6,065 ng/ml [IQR, 4,973–7,043 ng/ml], median 4,516 ng/ml [IQR, 3,972–5,304 ng/ml], and median 4,852 ng/ml [IQR, 4,069–8,612 ng/ml]); the differences between RPs versus healthy controls and chronic progressors versus healthy controls were significant ($P < 0.0001$) (Figure 5A). Additional plasma samples of the fourth VNP were consistently elevated. There was a trend toward increasing levels of sCD14 for individuals sampled at the time of advanced immunosuppression, with CD4+ T cell counts of below 350 cells/μl (Figure 5B).

Discussion

The current study defines 2 presentations of HIV infection that share a similar level of high viral replication but differ in the degree of immunological damage and in the pattern of clinical evolution, i.e., RPs and VNPs. The proportion of individuals with rapidly progressive disease was estimated in the SHCS (19). In this nationwide and representative cohort, 7.9% of HIV-infected individuals with a known seroconversion date fulfilled the criteria of RPs. Severity of the disease, rapid initiation of treatment, and the need for precise knowledge of the seroconversion window hampered recruitment of

RPs into clinical cohorts and research protocols in the past. VNPs constitute a group of individuals that sustain prolonged periods of high viral load, in the range of 100,000 copies/ml, while maintaining stable $CD4^+$ T cell counts. VNPs represent a very uncommon pattern of disease progression; prevalence estimates in the SHCS indicate that only 0.1% of HIV-infected individuals would fulfill the strict definition of VNPs used in the current work. However, the selected individuals likely represent the extreme of the distribution of VNPs, and relaxed criteria compared with those used in the present study will lead to different estimates of frequency.

The various genomic analyses in this study associate rapid progression with an enrichment for HLA alleles linked to adverse prognosis and a depletion of protective alleles. This pattern validates the phenotypic set of criteria elaborated to define rapid progression. In contrast, we found no association of the RP cohort with KIR alleles or KIR/HLA combinations previously related to disease progression or viremia (20). The genome-wide association study was conducted to exclude a major impact of common variants and to assess the candidates from a previous study of similar power (4) that could not be validated here. The transcriptome profile did confirm the deregulation of the ISGs in $CD8^+$ T cells in RPs, as previously documented for $CD4^+$ T cells (16, 21, 22) and in lymphatic tissue (23). It also identified a characteristic pattern of upregulation in $CD8^+$ T cells of RPs for genes involved in cell proliferation and cell division as well as in the immunoproteasome. RPs shared a number of features with the chronic SIV infection of rhesus macaques, in particular the prominent expression of a ISG and of immune activation markers. The absence of persistent immune activation during chronic SIV infection is a key characteristic of natural host species, such as the sooty mangabeys (24), and the presence of proliferation/activation markers on $CD4^+$ and $CD8^+$ T cells is an accurate predictor of disease in HIV-infected individuals (25). The immune activation gene set assessed in the present study was originally identified as being correlated with $CD8^+$ T cells expressing the activation marker Ki67 in SIV-infected rhesus macaques but was not expressed in SIV-infected sooty mangabeys (9).

More remarkable were the observations in VNPs. While the study did not have the power to allow a discovery that was not a priori, it permitted the assessment of a number of characteristics that have been previously described in SIV-infected sooty mangabeys. Individuals with the VNP profile display a limited deregulation of the ISG when compared with RPs, particularly in $CD8^+$ T cells. It should be stressed that these differences were present despite greater levels of viremia among VNPs than in RPs. In addition, to assess whether VNPs demonstrated lower immune activation and/or chronic interferon responses relative to RPs, we ranked the $CD4^+$ and $CD8^+$ expression data sets according to the significance value determined by the Bayesian analysis and used GSEA to test the relative position of ISGs/immune activation genes and genes differentially expressed in SIV-infected sooty mangabeys and rhesus macaques. This analysis supported the notion that the human profile of VNPs shares common features, at the transcriptome level, with the nonpathogenic model of SIV infection in the natural host. Reduced ISG expression is a consistent feature of natural host infection and not due to temporal fluctuation (10). Although the observation of reduced ISGs in VNPs in the current study is cross-sectional, it was consistent in showing ISG reduction relative to RPs. How differences in transcription levels of the ISGs translates into protein and the mechanisms of regulation should be the focus of future research (26).

We investigated in detail a set of genes identified through a comparative analysis of human and nonhuman primate transcriptome data; *CASP1*, *CD38*, *LAG3*, and *TNFSF13B* were upregulated in rhesus macaque and in human RPs; *SOCS1* and *EEF1D* were upregulated in sooty mangabeys and in human VNPs. The shared expression pattern between VNPs and sooty mangabeys supports their role in lentiviral pathogenesis. Caspase-1 precursor (CASP1) is a well-known intermediate of the inflammatory processes and apoptosis. The lymphocyte differentiation antigen CD38 is associated with immune exhaustion during immune activation and with adverse prognosis (27–29). LAG3 negatively regulates the expansion of activated T cells, and T cell homeostasis and is required for maximal regulatory T cell function (30) and has been demonstrated to associate with immune dysfunction/exhaustion of $CD8^+$ T cells in LCMV infection (31). Tumor necrosis factor ligand superfamily member 13B (TNFSF13B) is a receptor involved in the stimulation of B and T cell function and the regulation of humoral immunity. Suppressor of cytokine signaling (SOCS1) is involved in a negative feedback loop in the regulation of cytokine signal transduction signaled through the JAK/STAT5 pathway. Although *SOCS1* was downregulated in RPs compared with ECs and VNPs, its expression levels did not exhibit a significant association with viral set point or disease progression in the validation data set of $CD4^+$ T cell transcription data (16).

We completed the study by the analysis of a biomarker of compromised intestinal mucosal barrier, the monocyte-expressed LPS receptor sCD14 (18). Our data show higher plasma levels among RPs, in particular during advanced immunosuppression, than for other clinical progression groups. Although only 4 VNPs could be tested, 3 presented low sCD14 plasma levels, a pattern fitting other observations of lesser immunopathogenesis in these individuals. The transcriptome and biomarker data thus complement the work of Choudhary et al. (7) on VNPs that presented less extreme viral loads. They identified a lower percentage of activated $HLA\text{-}DR^+CD38^+CD4^+$ and $CD8^+$ T cells and lower levels of proliferating Ki67-expressing $CD4^+$ and $CD8^+$ T cells in VNPs compared with those of progressors. In contrast, viral isolates from VNPs and progressors replicated to similar levels and shared the capacity to deplete $CD4^+$ thymocytes or $CD4^+$ T cells in secondary lymphoid tissue and were equally cytopathic.

Future studies should extend analyses to plasmacytoid dendritic cells, as they are key activators of the immune system in HIV and SIV infection. Assessment of this cell population is limited by the low percentage of these cells in fresh blood, in particular, in the infected individual (32). The study has limited power due to the rarity of the study phenotypes and inherent limitations in recruitment. However, this work highlights the importance of 2 poorly understood clinical patterns of disease progression that have been minimally studied in the past and provides working definitions that should help identifying additional individuals to allow greater power in future genomic and functional studies. In addition, this report of a strong phenotypic similarity between nonpathogenic SIV infection of sooty mangabeys and a subset of HIV-infected individuals emphasizes the importance of studying natural SIV infection as a model to better understand HIV/AIDS pathogenesis.

Methods

Ethics statement. All participating centers provided local institutional review board approval for genetic analysis, and each participant provided informed consent for genetic testing. The Institutional Review Boards are

Comission d'Ethique de la Recherche Clinique, Faculté de Médecine, Université de Lausanne, Lausanne, Switzerland, and Comitè Etic d'Investigació Clínica, Hospital Germans Trias i Pujol, Badalona, Spain.

Patients and definition of clinical profiles. Study participants were followed in the SHCS (www.shcs.ch) or at the HIVACAT. The selection criteria for RPs included a HIV seroconversion window of less than 1 year with documented negative and positive serology and either of the following possibilities: (a) more than 2 $CD4^+$ T cell counts below 350 cells/μl within 3 years of seroconversion and no subsequent rise of $CD4^+$ T cells above 350/μl in the absence of combination antiretroviral therapy or (b) beginning antiretroviral therapy within 3 years of seroconversion and a $CD4^+$ T cell count within 1 month of starting antiretroviral therapy of less than 350/μl. $CD4^+$ T cell values in the first 6 months after seroconversion were excluded to avoid the $CD4^+$ T cell nadir during acute HIV infection.

The selection criteria of VNPs included more than 3 years of follow-up, median HIV viremia from more than 3 measurements of more than 100,000 cp/ml, HIV viremia consistently above 10,000 cp/ml, a $CD4^+$ T cell count above 350/μl, and no HIV treatment during follow-up.

Study candidates were identified by a standardized database search. Subsequently, the individual $CD4^+$ T cell profiles of all candidates were visually inspected before final inclusion. In addition to individuals fulfilling the definition of RP or of VNP, the study included 9 ECs as reference group.

Immunogenetic and genome-wide association analyses. High-resolution genotyping of *HLA-A*, *HLA-B*, *HLA-Cw*, and *DRB1* alleles was performed by sequence-based typing methods. *KIR* gene typing was performed by a sequence-specific oligonucleotide probe using the Luminex microbead technology. For genome-wide association analysis, participants were genotyped using Illumina BeadChips Human660W-Quad. For quality control purposes, SNPs were removed based on their absence (locus absence >5%), minor allele frequency (>1%), and Hardy-Weinberg Equilibrium deviation ($P < 1 \times 10^{-6}$). Participants were filtered based on call rate, gender check (heterozygosity testing), cryptic relatedness, and population structure (33).

Cell isolation, RNA extraction, and transcriptome profiling. For transcriptome analysis, we included all RPs ($n = 27$) for whom viable cells were available from the time of seroconversion (>6 months to 3 years from acute infection) and before initiation of antiretroviral treatment. Samples from all VNPs were included. The CD4 and viral load values at the time of transcriptome analysis are presented in Supplemental Table 1. $CD4^+$ and $CD8^+$ T cells were positively selected from frozen PBMCs (median time of cryopreservation was 1,485 [IQR, 821–2,558] days) using magnetically labeled $CD4^+$ or $CD8^+$ microbeads and subsequent column purification according to the manufacturer's protocol (Miltenyi Biotec). The median $CD4^+$ T cell purity, verified by flow cytometry, was 96.8% (range, 93.9%–98.9%), whereas the median $CD8^+$ T cell purity was 88.8% (range, 84.8%–92.1%). $CD4^+$ and $CD8^+$ T cell viability was assessed by the trypan blue dye exclusion method using the Vi-CELL (Beckman Coulter). Total RNA was extracted from purified $CD4^+$ and $CD8^+$ T cells using the mirVana miRNA Isolation Kit (Ambion) according to the manufacturer's protocol for total RNA extraction. The amount of RNA was estimated by spectrophotometry using the Nanodrop 1000 (Thermo Fisher). RNA quality was determined by the Agilent RNA 6000 Pico Kit on an Agilent 2100 Bioanalyzer. Samples were collected between 1993 and 2008 and investigated in 2009. The median of $CD4^+$ T cell viability for samples that were successfully analyzed was 79% (IQR, 64%–87%). The median of $CD8^+$ T cell viability for samples that were successfully analyzed was 82% (IQR, 74%–87%). Viability was minimally dependent on time of cryopreservation and more dependent on collection center. These covariates were assessed in the analyses. Target preparation was performed starting from 200 ng total RNA using the Illumina TotalPrep-96 RNA Amplification kit (Ambion). cDNA and cRNA were purified using the MagMAX Express Magnetic Particle Processor (Applied Biosystems). cRNA quality was assessed by capillary electrophoresis on the Agilent 2100 Bioanalyzer. Hybridization on HumanHT-12 v3 Expression BeadChips (Illumina) was carried out according to the manufacturer's instructions.

Transcriptome data analysis. Bead summary data were the output from Illumina's BeadStudio software without background correction, as this has previously been shown to have detrimental effects (34). Genes declared as nonexpressed ($P > 0.01$) were excluded from analysis. Data preprocessing, including quantile normalization and $\log_2$ transformation was completed in the Partek Genomics Suite package (Partek Inc.). Outliers were identified based on principal component analysis using 3 standard deviations as the cutoff for inclusion. For the differential expression analysis, we applied an empirical Bayes analysis approach, as implemented in the "limma" package of the R programming language, to model the variation profiles of all genes and used that information as prior knowledge to better estimate the variance of each gene expression (14).

The selected analysis included the following genes: *APOBEC3H*, *BST2*, *EIF2AK2*, *IFI27*, *IFI35*, *IFI44*, *IFIH1*, *IFITM1*, *IFITM3*, *IRF1*, *IRF9*, *ISG15*, *JAK1*, *JAK2*, *MX1*, *MX2*, *OAS3*, *STAT2*, *TAP*, *TRIM22*, *TYK2*, *ZBP1*, *APOBEC3F*, *APOBEC3G*, *IFI6*, *IFIT1*, *IFIT3*, *OAS1*, *OAS2*, *OASL*, *PSMB8*, *PTPN2*, *RNASEL*, *STAT1*, and *TRIM5* as previously described (16).

Signature analysis and validation. Because of the rarity of individuals with a VNP profile, we used a heuristic approach to assessing possible genetic markers associated with the clinical profile. This approach included the analysis of a preliminary signature, including genes identified as possibly associated with the VNP profile upon transcriptome analysis because of concordant signals in both $CD4^+$ and $CD8^+$ T cells as well as genes identified as potentially relevant in studies of SIV infection in the natural host: sooty mangabey and African green monkey. The signature was tested in an independent validation set of 153 individuals from a previous transcriptome analysis (16).

Pathway and network analyses. STRING (http://string.embl.de/) was used to identify known and predicted interactions (derived from 4 sources: genomic context, high-throughput experiments, coexpression, and previous knowledge). IPA (http://www.ingenuity.com/) and KEGG (http://www.genome.jp/kegg/pathway.html) were used for the analysis of pathway enrichment.

GSEA and gene set selection. The GSEA algorithm uses a Kolgorimov-Smirnov statistic to determine the significance of distribution of a set of genes within a larger, ranked data set (35). To evaluate the enrichment of SIV-inducible genes in the rhesus macaques and sooty mangabeys and in our human data set, we performed GSEA as follows: transcriptome data from VNPs and RPs were ranked according to their calculated Bayesian statistic; genes in which the mean was greater in VNPs were classified as positive, and genes with a greater mean in RPs were classified as negative. The data were ranked by the inverse Bayesian *P* value, resulting in a data set in which the most significant genes, overexpressed in VNPs, were listed at the top, and the most significant genes, overexpressed in RPs, were listing at the bottom. We next defined discrete query gene sets (Supplemental Table 6) from a large microarray data set, detailing longitudinal SIV infection in rhesus macaques, which develop disease, and sooty mangabeys, a nonpathogenic, natural host species, described previously (9). The ISG set comprised genes known to be regulated by type I interferon that were found to be differentially expressed in SIVmac239-infected rhesus macaques after 180 days of infection. The immune activation gene set was defined by multiple criteria: significant correlation of expression with lymphocyte activation assessed by circulating levels of $Ki67^+CD8^+$ T cells in SIVmac239-infected macaques (FDR = 0.0106), significant induction of expression assessed by ANOVA (FDR = 0.0075), a minimum of 2-fold upregulation in macaques at 1 or more time points, and expression in sooty mangabeys not exceeding 1.5× at any interval. To determine whether

gene expression maintained chronically in VNPs shared similarity with that of sooty mangabeys, we defined the sooty mangabey chronic query gene set as follows: robust multiarray average $\log_{10}$ intensity values from baseline samples were subtracted from chronic time points for individual animals of both species, and 2-sample *t* test was performed on the subsequent fold-change data; genes with a higher average fold change in sooty mangabeys relative to that in rhesus macaques were ranked according to *P* value, with the top 50 most significantly overexpressed genes selected for gene set inclusion. GSEA was performed using the desktop module available from the Broad Institute (www.broadinstitute.org/gsea/). GSEA was performed on the pre-ranked human data sets using 1,000 permutations, median collapse of duplicates, and random seeding.

Analysis of sCD14 levels. sCD14 levels were quantified in plasma samples using a commercially available ELISA assay (Diaclone). Plasma samples were diluted (1:50 or 1:100) and tested in duplicate. Plasma aliquots were collected either in EDTA ($n = 55$) or BD Vacutainer CPT Cell Preparation Tube with Sodium Citrate (CPT) tubes ($n = 12$). The CPT tubes contained a nonnegligible amount of molar sodium citrate solution (1 ml for the tubes, 8 ml draw capacity) and polysaccharide/sodium diatrizoate solution (FICOLL Hypaque solution; 2 ml for the tubes, 8 ml draw capacity), therefore samples collected with these tubes were considered to be diluted 1.44 times, and values were corrected accordingly.

Statistics. Comparisons of clinical and demographic characteristics used Fisher's exact tests for dichotomous variables and the Wilcoxon rank-sum test for continuous variables (STATA SE, release 11; StataCorp LP). In genome-wide association studies, association between genotype and phenotype (rapid progression) was tested using logistic regression, including top population principal components as covariates to correct for stratification. Genome-wide significance was assessed, using a cutoff of $P < 5 \times 10^{-8}$ to correct for multiple tests. In transcriptome analysis, we used a FDR method (36) to control for multiple testing. Probes selected for further analysis had an FDR-adjusted *P* value of less than 0.05. Statistical analyses dedicated to GSEA are detailed in the relevant section (see *GSEA and gene set selection*). Multiple regression analyses and graphical representations were performed by using the statistics package R (www.r-project.org).

Microarray data accession number. Microarray results have been deposited in the Gene Expression Omnibus database; the accession number is GSE28128.

Acknowledgments

This work has been financed in the framework of the SHCS and supported by the Swiss National Science Foundation (SNF) (grant no. 33CSC0-108787, project no. 587), by SNF grant (310000-110012, to A. Telenti), by the HIVACAT, and, in part, by the Ragon Institute and the Spanish AIDS network (RD06/0006). S.E. Bosinger is a recipient of a Canadian Institutes of Health Research HIV/AIDS Research Initiative Fellowship (HFE-85139). We thank S. Colombo, M. Rickenbach, I. Fernández, and J. Puig for study coordination; Y. Vallet for software support; John Wherry for the IA gene set; and E. Grau, R. Ayen, and T. González for technical assistance. The members of the SHCS are M. Battegay, E. Bernasconi, J. Böni, H.C. Bucher, Ph. Bürgisser, A. Calmy, S. Cattacin, M. Cavassini, R. Dubs, M. Egger, L. Elzi, P. Erb, M. Fischer, M. Flepp, A. Fontana, P. Francioli (President of the SHCS, Centre Hospitalier Universitaire Vaudois, CH-1011 Lausanne), H. Furrer (Chairman of the Clinical and Laboratory Committee), C. Fux, M. Gorgievski, H. Günthard (Chairman of the Scientific Board), H. Hirsch, B. Hirschel, I. Hösli, Ch. Kahlert, L. Kaiser, U. Karrer, C. Kind, Th. Klimkait, B. Ledergerber, G. Martinetti, B. Martinez, N. Müller, D. Nadal, M. Opravil, F. Paccaud, G. Pantaleo, A. Rauch, S. Regenass, M. Rickenbach (Head of Data Center), C. Rudin (Chairman of the Mother and Child Substudy), P. Schmid, D. Schultze, J. Schüpbach, R. Speck, P. Taffé, P. Tarr, A. Telenti, A. Trkola, P. Vernazza, R. Weber, and S. Yerly. The members of the HIVACAT involved in this study are B. Clotet, J. Dalmau, I. Erkizia, J.M. Gatell, C. Ligero, M. López-Diéguez, C. Manzardo, J. Martinez-Picado, and J.M. Miro.

Received for publication February 2, 2011, and accepted in revised form March 30, 2011.

Address correspondence to: Javier Martinez-Picado, AIDS Research Institute — IrsiCaixa, Hospital Germans Trias i Pujol, 08916 Badalona, Spain. Phone: 34.93.4656374; Fax: 34.93.4653968; E-mail: jmpicado@irsicaixa.es. Or to: Amalio Telenti, Institute of Microbiology, Bugnon 48, CHUV, 1011 Lausanne, Switzerland. Phone: 41.79.556.0751; Fax: 41.21.314.4095; E-mail: Amalio.telenti@chuv.ch.

1. Deeks SG, Walker BD. Human immunodeficiency virus controllers: mechanisms of durable virus control in the absence of antiretroviral therapy. *Immunity*. 2007;27(3):406–416.
2. Migueles SA, Connors M. Long-term nonprogressive disease among untreated HIV-infected individuals: clinical implications f understanding immune control of HIV. *JAMA*. 2010;304(2):194–201.
3. International HIV Controllers Study, et al. The major genetic determinants of HIV-1 control affect HLA class I peptide presentation. *Science*. 2010; 330(6010):1551–1557.
4. Le Clerc S, et al. Genomewide association study of a rapid progression cohort identifies new susceptibility alleles for AIDS (ANRS Genomewide Association Study 03). *J Infect Dis*. 2009;200(8):1194–1201.
5. Casado C, et al. Host and viral genetic correlates of clinical definitions of HIV-1 disease progression. *PLoS ONE*. 2010;5(6):e11079.
6. Dalmau J, et al. Contribution of immunological and virological factors to extremely severe primary HIV type 1 infection. *Clin Infect Dis*. 2009;48(2):229–238.
7. Choudhary SK, et al. Low immune activation despite high levels of pathogenic human immunodeficiency virus type 1 results in long-term asymptomatic disease. *J Virol*. 2007;81(16):8838–8842.
8. Lederer S, et al. Transcriptional profiling in pathogenic and non-pathogenic SIV infections reveals significant distinctions in kinetics and tissue compartmentalization. *PLoS Pathog*. 2009;5(2):e1000296.
9. Bosinger SE, et al. Global genomic analysis reveals rapid control of a robust innate response in SIV-infected sooty mangabeys. *J Clin Invest*. 2009; 119(12):3556–3572.
10. Jacquelin B, et al. Nonpathogenic SIV infection of African green monkeys induces a strong but rapidly controlled type I IFN response. *J Clin Invest*. 2009; 119(12):3544–3555.
11. Durudas A, Milush JM, Chen HL, Engram JC, Silvestri G, Sodora DL. Elevated levels of innate immune modulators in lymph nodes and blood are associated with more-rapid disease progression in simian immunodeficiency virus-infected monkeys. *J Virol*. 2009;83(23):12229–12240.
12. Taaffe J, et al. A five-year longitudinal analysis of sooty mangabeys naturally infected with simian immunodeficiency virus reveals a slow but progressive decline in CD4+ T-cell count whose magnitude is not predicted by viral load or immune activation. *J Virol*. 2010;84(11):5476–5484.
13. Moir S, Chun TW, Fauci AS. Pathogenic mechanisms of HIV disease. *Annu Rev Pathol*. 2011;6:223–248.
14. Smyth GK. Linear models and empirical bayes methods for assessing differential expression in microarray experiments. *Stat Appl Genet Mol Biol*. 2004; 3:Article3.
15. Haining WN, Wherry EJ. Integrating genomic signatures for immunologic discovery. *Immunity*. 2010; 32(2):152–161.
16. Rotger M, et al. Genome-wide mRNA expression correlates of viral control in CD4+ T-cells from HIV-1-infected individuals. *PLoS Pathog*. 2010; 6(2):e1000781.
17. Brenchley JM, et al. Microbial translocation is a cause of systemic immune activation in chronic HIV infection. *Nat Med*. 2006;12(12):1365–1371.
18. Sandler NG, et al. Plasma levels of soluble CD14 independently predict mortality in HIV infection. *J Infect Dis*. 2011;203(6):780–790.
19. Swiss HIV Cohort Study, et al. Cohort profile: the Swiss HIV Cohort study. *Int J Epidemiol*. 2010; 39(5):1179–1189.
20. Carrington M, Martin MP, van Bergen J. KIR-HLA intercourse in HIV disease. *Trends Microbiol*. 2008; 16(12):620–627.
21. Hyrcza MD, et al. Distinct transcriptional profiles in ex vivo CD4+ and CD8+ T cells are established early in human immunodeficiency virus type 1 infection and are characterized by a chronic interferon response as well as extensive transcriptional changes in CD8+ T cells. *J Virol*. 2007;81(7):3477–3486.
22. Sedaghat AR, et al. Chronic CD4+ T-cell activation and depletion in human immunodeficiency virus type 1 infection: type I interferon-mediated disruption of T-cell dynamics. *J Virol*. 2008;82(4):1870–1883.
23. Smith AJ, Li Q, Wietgrefe SW, Schacker TW, Reilly CS, Haase AT. Host genes associated with

HIV-1 replication in lymphatic tissue. *J Immunol*. 2010;185(9):5417–5424.
24. Silvestri G, et al. Nonpathogenic SIV infection of sooty mangabeys is characterized by limited bystander immunopathology despite chronic high-level viremia. *Immunity*. 2003;18(3):441–452.
25. Giorgi JV, et al. Shorter survival in advanced human immunodeficiency virus type 1 infection is more closely associated with T lymphocyte activation than with plasma virus burden or virus chemokine coreceptor usage. *J Infect Dis*. 1999;179(4):859–870.
26. Witwer KW, Sisk JM, Gama L, Clements JE. MicroRNA regulation of IFN-beta protein expression: rapid and sensitive modulation of the innate immune response. *J Immunol*. 2010;184(5):2369–2376.
27. Biancotto A, et al. Abnormal activation and cytokine spectra in lymph nodes of people chronically infected with HIV-1. *Blood*. 2007;109(10):4272–4279.
28. Onlamoon N, Tabprasit S, Suwanagool S, Louisirirotchanakul S, Ansari AA, Pattanapanyasat K. Studies on the potential use of CD38 expression as a marker for the efficacy of anti-retroviral therapy in HIV-1-infected patients in Thailand. *Virology*. 2005;341(2):238–247.
29. Li Q, et al. Microarray analysis of lymphatic tissue reveals stage-specific, gene expression signatures in HIV-1 infection. *J Immunol*. 2009;183(3):1975–1982.
30. Workman CJ, Dugger KJ, Vignali DA. Cutting edge: molecular analysis of the negative regulatory function of lymphocyte activation gene-3. *J Immunol*. 2002;169(10):5392–5395.
31. Blackburn SD, et al. Coregulation of CD8+ T cell exhaustion by multiple inhibitory receptors during chronic viral infection. *Nat Immunol*. 2009; 10(1):29–37.
32. Brown KN, Wijewardana V, Liu X, Barratt-Boyes SM. Rapid influx and death of plasmacytoid dendritic cells in lymph nodes mediate depletion in acute simian immunodeficiency virus infection. *PLoS Pathog*. 2009;5(5):e1000413.
33. Price AL, Patterson NJ, Plenge RM, Weinblatt ME, Shadick NA, Reich D. Principal components analysis corrects for stratification in genome-wide association studies. *Nat Genet*. 2006;38(8):904–909.
34. Dunning MJ, Barbosa-Morais NL, Lynch AG, Tavaré S, Ritchie ME. Statistical issues in the analysis of Illumina data. *BMC Bioinformatics*. 2008;9:85.
35. Subramanian A, et al. Gene set enrichment analysis: a knowledge-based approach for interpreting genome-wide expression profiles. *Proc Natl Acad Sci U S A*. 2005;102(43):15545–15550.
36. Benjamini Y, Hochberg Y. Controlling the false discovery rate: a practical and powerful approach to multiple testing. *J R Statist Soc B*. 1995;57(1):289–289.